Graphical abstract for the table of contents entry

The *n*-doped poly(phenanthrenequinone) is electrically conductive to be successfully used as the binder for nano-silicon negative electrodes.

Energy & Environmental Science

Poly(phenanthrenequinone) as a Conductive Binder for Nano-sized Silicon Negative Electrodes†

Sang-Mo Kim,‡[a] Myeong Hak Kim,‡[a] Sung Yeol Choi,[a] Jae Gil Lee,[a] Jihyun Jang,[a] Jeong Beom Lee,[a] Ji Heon Ryu,[b] Seung Sik Hwang,[c] Jin-Hwan Park,[c] Kyusoon Shin,[d] Young Gyu Kim*[a] and Seung M. Oh*[a]

3,6-Poly(phenanthrenequinone) (PPQ) is synthesized and tested as a conductive binder. The PPQ binder, formulated with nano-sized Si powder without conductive carbon, is *n*-doped by accepting electrons and Li$^+$ ions to become a mixed conductor in the first charging period. The resulting *n*-doped PPQ binder remains conductive thereafter within the working potential of Si (0.0~0.5 V *vs.* Li/Li$^+$). Within the composite electrode, the PPQ binder is uniformly dispersed to effectively convey electrons from the current collector to the Si particles. Namely, the PPQ binder by itself plays the roles of conductive carbon and polymer binder that are loaded in the conventional composite electrodes. Due to the highly conductive nature, the loading of PPQ binder can be minimized down to 10 wt. %, which is close to that used for practical electrode formulation, with reasonable rate and cycle performances for the nano-Si electrode.

Introduction

Over the last decades, graphite has been the most popularly used negative electrode since this crystalline carbon largely meets the requirements imposed on the negative electrodes of lithium-ion batteries (LIBs).[1–3] The market of LIBs is now expanding to electric vehicles (EVs) and energy storage systems (ESSs). However, because of the limited specific capacity for graphite, the alternatives having higher specific capacity have been highly sought. Silicon (theoretical capacity = 3579 mA h g$_{Si}^{-1}$) has emerged as a viable candidate.[4–7] The practical use of Si is, however, still hindered because of a critical problem that is associated with massive volume change upon cycling. The volume change frequently leads to a formation of cracks or pulverization of Si particles, which eventually causes a breakdown of electrically conductive network made between Si particles, conductive carbon particles and metallic current collector. To solve or at least mitigate this volume-change problem, many efforts have been made including the nano-structuring of Si[8–11] and introduction of a buffer matrix.[12-19] The nano-sizing approach seems promising because the absolute volume change can be reduced.[20] However, another issue has emerged in this approach, which is the excessive loading of conductive carbon and polymeric binder. Namely, a large amount of conductive carbon is needed to make electric contacts with nano-sized Si particles because the surface area of nano-Si is much larger than that for the bulk-

sized ones. Moreover, the use of an excessive amount of polymeric binder is inevitable in binding such a large number of Si and carbon particles. The loading of a large amount of inactive components (conductive carbon and polymeric binder) results in a decrease in the energy density of LIBs.

This work was motivated by a simple premise that the electrically conductive network can be made without conductive carbon if the polymeric binder itself is electrically conductive. That is, if this is possible, the conductive polymer by itself serves as both the conductive carbon and polymeric binder to minimize the loading of inactive components in the electrode layer. To implement this premise, the following points should further be considered. First, the candidate polymer should be electronically conductive within the working potential of Si (0.0~0.5 V *vs.* Li/Li$^+$) to serve as the electron transfer channel between the Si particles and the current collector. Second, the polymer should be uniformly dispersed with a strong binding ability within the electrode layer. Third, the loading of conductive polymer binder should be minimized to maximize the energy density of the cells. The *p*-type conducting polymers such as polyaniline and polypyrrole are discarded in this work because they are electronically conductive only at >3.0 V (*vs.* Li/Li$^+$).[21]

In this work, a polymer derived from 9,10-phenanthrenequione (PQ) was synthesized and tested to determine whether it satisfies the above-mentioned requirements. The selection of PQ was based on its unique

molecular structure. Namely, the conductive polymers to be employed as the binder for Si negative electrodes should have a very low value in the lowest unoccupied molecular orbital (LUMO), such that they are readily reduced by *n*-doping to be electronically conductive in the working potential of Si. PQ seems to be one of the right choices because it is highly conjugated and has the electron-withdrawing carbonyl group.[22] Furthermore, the *n*-doping by two electrons/Li$^+$ ions per formula unit is possible due to the presence of two carbonyl substituents. One can assume a high electronic conductivity on the basis of the molecular structure.

To assess the binder performance of PPQ, a composite electrode was prepared from a mixture of nano-sized Si powder and the conducting polymer (PPQ) without conductive carbon, and its electrode performances were examined. For comparison purposes, another composite electrode was prepared with poly(acrylic acid) lithium salt (LiPAA), which is a non-conductive binder.

Experimental section

Synthesis of poly(phenanthrenequinone)

The details on the monomers and synthetic procedure are given in ESI† (Fig. S1). 3,6-Poly(phenanthrenequinone) (PPQ) was synthesized by using the Suzuki coupling reaction.[23] In detail, a solution of 3,6-dibromophenanthrene-9,10-dione (compound **1** in Fig. S1) (0.50 g, 1.52 mmol) and 3,6-bis(4,4,5,5,-tetramethyl-1,3,2-dioxaborolan-2-yl)phenanthrene-9,10-dione (compound **2** in Fig. S1) (0.70 g, 1.52 mmol) in toluene (80 mL) and THF (20 ml) was stirred in round flask. Then, Pd(PPh$_3$)$_4$ (15.6 mg, 0.15 mmol), Na$_2$CO$_3$ (2 ml, 2.0 M in distilled water) and Aliquat 336 (1 ml) as a phase transfer catalyst were added. The reaction mixture was stirred vigorously for 2 days at 110°C, and the resulting crude mixture was concentrated by rotary evaporator and precipitated in methanol/H$_2$O/1.0 N HCl mixture (ratio of 10/10/1 v/v).[22–24] The precipitate was centrifuged and dried in air. The dried polymer was fractionated by soxhlet extraction with methanol and dichloromethane. Residue deep brownish solid was collected and dried under vacuum. GPC (DMF, PMMA standard): M_n = 5900, M_w = 6138, M_w/M_n = 1.04.

Electrochemical characterizations

To examine the electrochemical performances of PPQ itself, a composite PPQ electrode was fabricated. To this end, PPQ was dissolved in *N*-methyl-2-pyrrolidone (NMP, anhydrous, 99.5 %), and the resulting viscous solution was dispersed on a piece of Cu foil (current collector) and dried at 120°C. The PPQ is deposited as a film on Cu foil.

Two different nano-Si composite electrodes were prepared by using either PPQ or LiPAA as the binder. For the nano-Si/PPQ composite electrode, PPQ was dissolved into NMP, into which nano-sized Si powder (crystalline, APS ≤ 50 nm, 98 %, laser synthesized from vapor phase, Alfa Aesar) was dispersed. The resulting slurry was coated on a piece of Cu foil and dried

at 120°C. The PPQ loading was varied at 10~30 wt. %. For the nano-Si/LiPAA composite electrode, poly(acrylic acid) (PAA, average Mv ~ 450000) and lithium hydroxide (LiOH, ACS reagent, ≥ 98.0 %) were dissolved into distilled water, into which the nano-Si powder was dispersed. The resulting slurry was coated on a piece of Cu foil and dried at 120°C. The LiPAA loading was varied at 10~30 wt. %. Si loading in the composite electrodes was 0.46 mg cm^{-2} for Si-LiPAA (7:3), 0.55 mg cm^{-2} for Si-PPQ (7:3) and 0.70 mg cm^{-2} for Si-PPQ (9:1), respectively. Electrode thickness was 9 μm for Si-LiPAA (7:3), 12 μm for Si-PPQ (7:3) and Si-PPQ (9:1), respectively. Electrode porosity was 65 % for Si-LiPAA, 69 % for Si-PPQ (7:3) and 70 % for Si-PPQ (9:1), respectively.

To examine the electrochemical performances of PPQ itself, a Li/PPQ cell (2032 coin-type, electrode diameter = 11 mm) was fabricated with lithium foil (as a counter and reference electrode), and polypropylene (PP)/polyethylene (PE)/PP tri-layer separator. The used electrolyte was 1.0 *M* LiPF$_6$ dissolved in ethylene carbonate (EC)/diethyl carbonate (DEC) (1:1, vol. ratio). Li/nano-Si cells (2032 coin-type) were also fabricated to characterize the electrode performance of nano-sized Si electrodes. To this end, the nano-Si/PPQ and nano-Si/LiPAA composite electrodes were loaded into the coin cells along with Li foil. The used electrolyte was 1.3 *M* LiPF$_6$ dissolved in EC/fluoroethylene carbonate (FEC)/DEC (2:2:6, vol. ratio). The PP/PE/PP tri-layer separator was used.

The galvanostatic lithiation (discharge) and de-lithiation (charge) cycling of Li/PPQ and Li/nano-Si cells were conducted using a TOSCAT-3100 (TOYO SYMSTEM CO., LTD.) at 25°C in a constant current-constant voltage (CC-CV) mode. In the case of Li/PPQ cell, the current density was 100 mA g$_{PPQ}$$^{-1}$ and the voltage cut-off was 0.005~3.0 V (*vs.* Li/Li$^+$). Before the charge-discharge cycling, the Li/nano-Si cells were cycled twice at a current density of 100 mA g$_{Si}$$^{-1}$ over the potential range of 0.005~1.0 V. In this work, the initial two-cycling is denoted as "pre-cycling". The cycle number is counted from the following lithiation/de-lithiation. The current density was fixed at 358 mA g$_{Si}$$^{-1}$ (0.1 C-rate) to characterize the Li/nano-Si cell performances. For the rate capability test, the de-lithiation current was varied from 0.1 C to 3 C after the pre-cycling while the lithiation current being fixed at 0.1 C.

Galvanostatic intermittent titration technique (GITT) was employed to monitor the evolution of internal resistance upon cycling in the Li/nano-Si cells. To this end, a series of current pulse (0.1 C for 10 min) and rest (for 30 min) was applied over the potential range of 0.005~1.0 V. In each rest period, the cell voltage was traced by using a battery cycler (WBCS3000) at 25°C. The voltage value right after the current pulse and at the end of rest was taken in each current pulse as a closed-circuit voltage (CCV) and quasi-open-circuit voltage (QOCV), respectively, from which the cell polarization is calculated as the difference between the end of CCV and QOCV. The internal resistance of the cells was then calculated by the following relation[25]: Internal resistance (Ω) = Cell polarization (V) / Applied current (A).

Morphology characterization

Morphology of the composite electrodes was observed with transmission electron microscopy (TEM). TEM measurement was performed using JEM-ARM200F (JEOL Ltd., Japan) operated at 200 kV. In order to identify the polymer from the composite, imaging with bright-field scanning TEM (BF-STEM) and elemental mapping with energy dispersive x-ray spectroscopy (EDS) were performed. Samples were prepared by dropping the nano-Si/polymer binder composite onto a lacey carbon-coated Cu grid and drying overnight under vacuum.

Results and discussion

Galvanostatic charge-discharge voltage profiles of the Li/nano-Si cell fabricated with two different polymer binders are shown in Fig. 1a and the corresponding differential capacity (dQ/dV) plots are provided in Fig. 1b. The reversible capacity in the first cycle is compared for the two Li/nano-Si electrodes in Fig. 1a. The first de-lithiation capacity delivered by the nano-Si electrode with the LiPAA binder is much smaller (2471 mA h g_{Si}^{-1}) than the theoretical value (3579 mA h g_{Si}^{-1}) even if the charge/discharge rate is very slow (0.028 C), illustrating that all the nano-Si particles are not utilized for lithiation/de-lithiation. Such an incomplete utilization is ascertained with a control experiment, in which carbon black (Super P) is added into this electrode as a conductive agent and cycled in the same condition. As seen in Fig. S2, the de-lithiation capacity now increases up to 2883 mA h g_{Si}^{-1}, showing that the utilization of nano-Si particles increases due to the reinforcement of the electrically conductive network by the presence of carbon black. When LiPAA is replaced by the PPQ binder, however, the nano-Si electrode delivers a de-lithiation capacity of 3271 mA h g_{Si}^{-1} at the same rate (0.028 C), which is 91 % of the theoretical value. This feature ensures that continuous current paths are made in the latter electrode even without carbon black due to the electrically conducting role of PPQ binder.[26]

To confirm the conducting role of PPQ, the PPQ by itself is deposited on Cu foil as a film and the resulting Li/PPQ cell is charge/discharge cycled (Fig. 1c). In this cell, the PPQ film is lithiated up to 1239 mA h g_{PPQ}^{-1} in the first cycle but de-lithiated to 372 mA h g_{PPQ}^{-1}. The large lithiation capacity at about 0.15 V in the first cycle shows that the PPQ film takes electric charges of 1239 mA h g_{PPQ}^{-1} and the equivalent amount of Li$^+$ ions. That is, the PPQ film is n-doped by taking electrons and Li$^+$ ions in this potential region: the PPQ film becomes mixed-conducting like the electrode materials used in lithium-ion batteries. The much smaller first de-lithiation capacity implies that large amount of electrons/Li$^+$ ions are trapped inside the PPQ matrix. This trapping is undesirable in one sense because it causes an irreversible capacity when used as the binder. Hence, the PPQ loading should be minimized. However, the Li trapping is beneficial in the other sense because PPQ maintains its mixed-conducting property once it is lithiated in the first cycle.

The n-doping for the PPQ binder that is formulated with the nano-Si powder is confirmed in Fig. 1d, in which the first

differential lithiation capacity plot of the Li/nano-Si cell (with PPQ binder) is magnified. A shoulder (0.1~0.15 V) overlaps the lithiation peak of Si. The shoulder must be responsible for the lithiation of PPQ binder because it does not appear with LiPAA binder. In addition, the position of shoulder is very close to the lithiation peak for the pure PPQ film electrode (0.15~0.18 V). The slight shift to the negative potential (polarization) must be due to the presence of less conductive Si particles in the nano-Si/PPQ composite electrode. In short, the PPQ binder in the composite electrode becomes electrically conductive by n-doping in the first cycle and plays the conducting role thereafter.

To highlight the conducting role of the PPQ binder, a rate test is performed with two nano-Si composite electrodes fabricated with two binders. The electrode fabricated with the PPQ binder outperforms the other one with respect to rate property (Fig. 2). The de-lithiation capacity difference of two electrodes is not big at a slower rate (0.1 C), but becomes larger with an increase in the de-lithiation current. At 3 C (ca. 10 A g_{Si}^{-1}), the nano-Si electrode with PPQ binder delivers a de-lithiation capacity up to 2362 mA h g_{Si}^{-1}, contrasted by the electrode prepared with LiPAA which delivers 439 mA h g_{Si}^{-1} at the same rate. This means that the electrically conductive network is well-made with the PPQ binder, which is not the case with the LiPAA binder. The internal resistance of two electrodes is compared to show the differences in the conducting role of two binders. The Li/nano-Si cell with LiPAA shows a decrease in the internal resistance from 0.3 V in the lithiation period (Fig. 3b), which is due to a decrease in contact resistance at the particle-to-particle and/or particle-to-current collector contacts, caused by the volume expansion of the Si particles.[25] In the de-lithiation period, the internal resistance rapidly increases from 0.4 V due to contact loss caused by volume contraction of Si particles. The evolution of internal resistance with PPQ binder is, however, quite different to that observed with LiPAA. The internal resistance is already marginal before the major lithiation of Si takes place at ca. 0.3 V, from which the contact resistance is supposed to be reduced due to the expansion of Si particles. This implies that the electrically conductive network is already well-made during the pre-cycling stage. In the forthcoming de-lithiation, the internal resistance increases from 0.4 V due to Si contraction but to a much lesser degree than that observed with LiPAA binder. A practical important feature here is that the internal resistance remains marginal at 0.0~0.5 V, within which the Si electrode is charged/discharged.

As mentioned in the introduction, it is necessary for any conducting polymer binders to be uniformly dispersed within the electrode layer to effectively play a conducting role. Fig. 4 shows the TEM images of two composite electrodes. The positions of Si and polymers can be identified from the elemental mapping of Si (Fig. 4d and 4h) and carbon (Fig. 4c and 4g). As is seen in the fig. 4a~4d, the nano-Si particles are fully covered by the LiPAA layer, which is known as a surface-covering binder.[27,28] A similar full coverage of nano-Si by PPQ is observed in Fig. 3e~3h. Such uniform coverage by the

conductive PPQ layer offers effective current paths between the whole Si surface and the current collector allowing high utilization of Si particles and enabling high-rate charge/discharge for this electrode. When the insulating LiPAA binder is used, however, the current paths are formed only through the Si particle-to-particle contacts; therefore, the electrode resistance is large.

Fig. 5 presents the cycle performance of two Li/nano-Si cells along with the Coulombic efficiency. The nano-Si electrode fabricated with 30 wt. % of PPQ shows a de-lithiation capacity of 3258 mA h g_{Si}^{-1} in the first cycle and 2823 mA h g_{Si}^{-1} in the 50th cycle, which is larger than those for the electrode fabricated with 30 wt. % of LiPAA. The larger capacity of the former electrode must be because of the almost full utilization of the Si particles due to the well-developed current paths. The reasonably good cycle retention explains the electrochemically stable nature of the PPQ binder. A binder content of 30 wt. % is far from practical because of its massive volume occupation by light-weight polymers. In the case of PPQ binder, the minimization of binder loading is even more important because PPQ causes an irreversible capacity (Fig. 1c). Along this line, the PPQ loading is decreased to 10 wt. %, which is close to that used for practical electrode formulations. As is seen in Fig. 5, the delivered capacity and cycleability are a little poorer with 10 wt. % loading, showing that the electrically conductive network is not perfect. However, the electrode performance is still impressive.

The evolution of Coulombic efficiency for three Si composite electrodes is presented in Fig. 5b. All the Si electrodes show a Coulombic efficiency of less than 97 % in the pre-cycling stage (initial two cycles), but the values are retained at >97 % thereafter. In the case of the nano-Si electrode fabricated with 30 wt. % of PPQ (Si:PPQ = 7:3), the Coulombic efficiency is as low as 70 % in the first cycle during the pre-cycling step due to large irreversible capacity. Two origins can be assumed for the irreversible capacity. One is the uptake of Li^+ ions/electrons by the PPQ binder in the first lithiation period (Fig. 1c) and the other is the consumption of Li^+ ions/electrons for the reductive electrolyte decomposition on the Si electrode surface. Note that the used Si is nano-sized (surface area = 57 $m^2 g^{-1}$), such that the second contribution seems to be appreciable. This feature is ensured by the observation that the first Coulombic efficiency is 82 % for Si:LiPAA = 7:3, in which only the electrolyte decomposition prevails since Li trapping is absent for LiPAA binder. Meanwhile, the Si:PPQ = 9:1 composite electrode, in which the PPQ loading was reduced to mitigate the contribution from the Li trapping by PPQ binder, gives a Coulombic efficiency of 81 % in the first pre-cycle, which is comparable to that observed with Si:LiPAA = 7:3 (82 %). Presumably, the irreversible capacity that is associated with the electrolyte decomposition is dominant over that coming from Li trapping in the Si:PPQ = 9:1 composite electrode. A simple calculation, which was performed on the basis of Li trapping by PPQ (Fig. 1c) and the theoretical capacity of Si (3579 mA h g_{Si}^{-1}), shows that the Li trapping by PPQ binder in Si:PPQ = 9:1 electrode is 87 mA h

g_{total}^{-1}, which is marginal as compared to the capacity delivered by the Si component (3221 mA h g_{total}^{-1}). Here, the subscript "total" means the sum of the weight of Si and PPQ binder. This feature manifests itself that the irreversible capacity caused by Li trapping can be reduced by decreasing the PPQ loading in the composite electrode as far as the electrode performance is not seriously deteriorated.

Another way to prevent the irreversible capacity caused by Li trapping is the use of pre-lithiated PPQ binder. Namely, if PPQ can be lithiated by chemical or electrochemical methods, and the pre-lithiated PPQ is chemically stable at ambient conditions, it can be added as a binder through the conventional slurry preparation method. Unfortunately, the pre-lithiated PPQ by electrochemical reaction exhibits a poor solubility in the common organic solvents. Furthermore, the pre-lithiated PPQ loses the mixed conducting behavior once it is exposed to ambient conditions, probably due to the reactions with moisture water and oxygen.

Conclusions

This work tests whether PPQ could act as a conductive binder. The results show a high feasibility for this premise because PPQ largely meets the requirements. First, PPQ is *n*-doped to be a mixed conductor during the first lithiation period. The binder is electronically conductive in the working potential of Si (0.0~0.5 V). Second, the PPQ binder is uniformly dispersed within the nano-Si composite electrode to effectively convey electrons from Si to the current collector. Finally, the loading of PPQ can be minimized down to 10 wt. %.

Acknowledgements

Notes and references

[a] Department of Chemical and Biological Engineering, Seoul National University, Seoul 151-744, Korea. E-mail: ygkim@snu.ac.kr, seungoh@snu.ac.kr

[b] Graduate School of Knowledge-based Technology and Energy, Korea Polytechnic University, Siheung-si, Korea.

[c] Energy Lab, Samsung Advanced Institute of Technology, Samsung Electronics, 560 Maetan-dong, Suwon, Korea.

[d] Dongjin Semichem Co., 613 Sampyungdong, Bundanggu, Seongnamsi, Gyeonggido, 463-400, Korea.

† Electronic Supplementary Information (ESI) available: The details on the monomers and synthetic procedure (Fig. S1), and the charge/discharge voltage profiles of Li/nano-Si cell fabricated with LiPAA binder (Fig. S2). See DOI: 10.1039/b000000x/
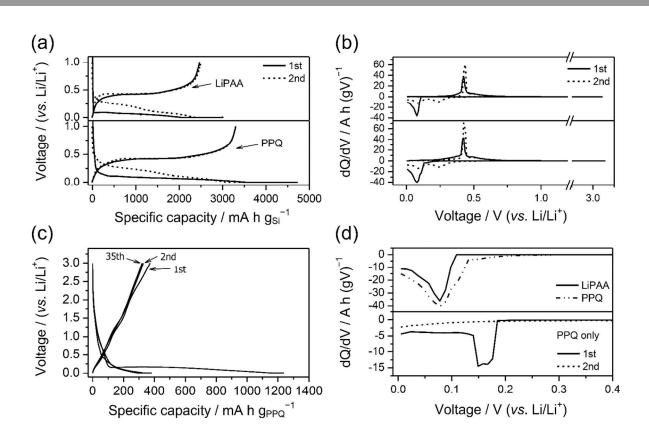
‡ These authors contributed equally to this work.

1   J. R. Dahn, T. Zheng, Y. Liu and J. S. Xue, *Science*, 1995, **270**, 590–593.

2   R. Fong, U. von Sacken and J. R. Dahn, *J. Electrochem. Soc.*, 1990, **137**, 2009–2013.

3   C. Wang, A. J. Appleby and F. E. Little, *J. Electroanal. Chem.*, 2001, **497**, 33–46.

4   T. D. Hatchard and J. R. Dahn, *J. Electrochem. Soc.*, 2004, **151**, A838–A842.

5   M. N. Obrovac and L. Christensen, *Electrochem. Solid-State Lett.*, 2004, **7**, A93–A96.

6   M. N. Obrovac and L. J. Krause, *J. Electrochem. Soc.*, 2007, **154**, A103–A108.

7   T. Takamura, S. Ohara, M. Uehara, J. Suzuki and K. Sekine, *J. Power Sources*, 2004, **129**, 96–100.

8   H. Kim, M. Seo, M.-H. Park and J. Cho, *Angew. Chem. Int. Ed.*, 2010, **49**, 2146–2149.

9   B. Laïk, L. Eude, J.-P. Pereira-Ramos, C. S. Cojocaru, D. Pribat and E. Rouvière, *Electrochim. Acta*, 2008, **53**, 5528–5532.

10 H. Li, X. Huang, L. Chen, Z. Wu and Y. Liang, *Electrochem. Solid-State Lett.*, 1999, **2**, 547–549.

11 K. Peng, J. Jie, W. Zhang and S.-T. Lee, *Appl. Phys. Lett.*, 2008, **93**, 033105.

12 S. Chen, M. L. Gordin, R. Yi, G. Howlett, H. Sohn and D. Wang, *PCCP*, 2012, **14**, 12741–12745.

13 S. Iwamura, H. Nishihara and T. Kyotani, *J. Phys. Chem. C*, 2012, **116**, 6004–6011.

14 J.-H. Kim, H.-J. Sohn, H. Kim, G. Jeong and W. Choi, *J. Power Sources*, 2007, **170**, 456–459.

15 T. Kim, S. Park and S. M. Oh, *J. Electrochem. Soc.*, 2007, **154**, A1112–A1117.

16 H. Wu, G. Zheng, N. Liu, T. J. Carney, Y. Yang and Y. Cui, *Nano Lett.*, 2012, **12**, 904–909.

17 Z. Y. Zeng, J. P. Tu, Y. Z. Yang, J. Y. Xiang, X. H. Huang, F. Mao and M. Ma, *Electrochim. Acta*, 2008, **53**, 2724–2728.

18 X. N. Zhang, G. L. Pan, G. R. Li, J. Q. Qu and X. P. Gao, *Solid State Ionics*, 2007, **178**, 1107–1112.

19 P. Zuo and G. Yin, *J. Alloys Compd.*, 2006, **414**, 265–268.

20 M. Winter and J. O. Besenhard, *Electrochim. Acta*, 1999, **45**, 31–50.

21 P. Novák, K. Müller, K. S. V. Santhanam and O. Haas, *Chem. Rev.*, 1997, **97**, 207–282.

22 G. Liu, S. Xun, N. Vukmirovic, X. Song, P. Olalde-Velasco, H. Zheng, V. S. Battaglia, L. Wang and W. Yang, *Adv. Mater.*, 2011, **23**, 4679–4683.

23 W. Vanormelingen, A. Smeets, E. Franz, I. Asselberghs, K. Clays, T. Verbiest and G. Koeckelberghs, *Macromolecules*, 2009, **42**, 4282–4287.

24 C. Yang, H. Scheiber, E. J. W. List, J. Jacob and K. Müllen, *Macromolecules*, 2006, **39**, 5213–5221.

25 J. H. Ryu, J. W. Kim, Y.-E. Sung and S. M. Oh, *Electrochem. Solid-State Lett.*, 2004, **7**, A306–A309.

26 M. Wu, X. Xiao, N. Vukmirovic, S. Xun, P. K. Das, X. Song, P. Olalde-Velasco, D. Wang, A. Z. Weber, L.-W. Wang, V. S. Battaglia, W. Yang and G. Liu, *J. Am. Chem. Soc.*, 2013, **135**, 12048–12056.

27 S. Komaba, K. Okushi, T. Ozeki, H. Yui, Y. Katayama, T. Miura, T. Saito and H. Groult, *Electrochem. Solid-State Lett.*, 2009, **12**, A107–A110.

28 S. Komaba, K. Shimomura, N. Yabuuchi, T. Ozeki, H. Yui and K. Konno, *J. Phys. Chem. C*, 2011, **115**, 13487–13495.

Energy & Environmental Science

ARTICLE

Fig. 1. (a); The charge/discharge voltage profiles of Li/nano-Si cells fabricated with two different binders in the initial two cycles (pre-cycling stage), (b); the corresponding differential capacity (dQ/dV) plots, (c); the charge/discharge voltage profiles of Li/PPQ cell, and (d); the magnified view of the first differential lithiation capacity plots of Li/nano-Si cells and Li/PPQ cell. The binder content in the nano-Si composite electrode was 30 wt. %. Current density = 100 mA g_{Si}^{-1} (0.028 C).
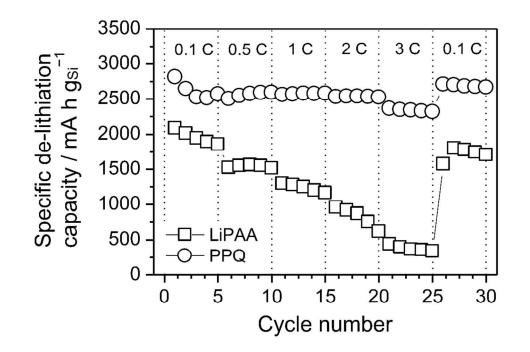
Fig. 2. Rate capability of Li/nano-Si cells with two binders (30 wt. %). The de-lithiation current is indicated. For the lithiation, a constant current (CC) mode was used at 0.1 C.
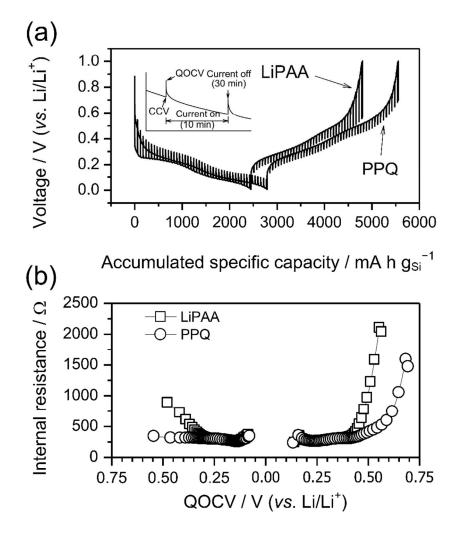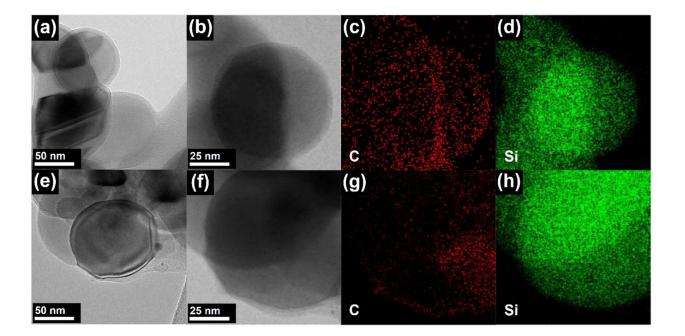
Fig. 3. (a); The transient voltage profiles obtained from galvanostatic intermittent titration technique and (b); the evolution of internal resistance derived from the difference between the end of closed-circuit-voltage (CCV) and the quasi-open-circuit-voltage (QOCV). The GITT experiment was carried out after two charge/discharge cycles (pre-cycling).

Fig. 4. TEM images of the nano-Si/polymer binder composites: (a~d); LiPAA and (e~h); PPQ. The bright-field STEM images and their EDS maps: (b~d); LiPAA and (f~h); PPQ. The red and green dots represent C and Si, respectively.
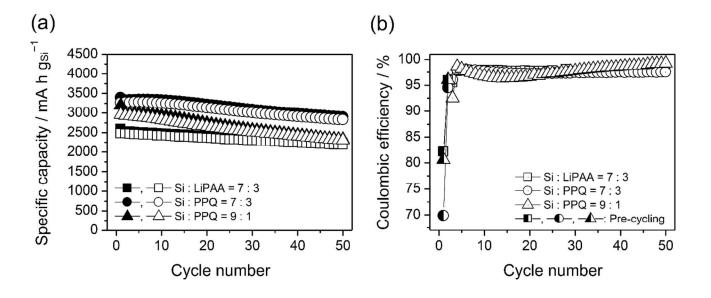
Energy & Environmental Science Accepted Manuscript

(a)

(b)

Fig. 5. (a); Cycle performance of Li/nano-Si cells (pre-cycling data are excluded). The filled and empty symbols indicate the lithiation and de-lithiation capacity, respectively. Note that the capacity values are larger than those in Fig. 2 because a constant current (CC at 0.1 C) and constant voltage (CV) mode was used for this data. A constant current (CC at 0.1 C) mode was used for Fig. 2. (b); Coulombic efficiency of Li/nano-Si cells. The half-filled symbols indicate the Coulombic efficiency in the initial two cycles (pre-cycling).